Differential Expression of Inflammatory Cytokines Parallels Progression of Central Nervous System Pathology in Two Clinically Distinct Models of Multiple Sclerosis[1]

Wendy Smith Begolka, Carol L. Vanderlugt, Sandra M. Rahbe, and Stephen D. Miller[2]

Multiple sclerosis is an immune-mediated demyelinating disease of unknown etiology that presents with either a chronic-progressive or relapsing-remitting clinical course. Theiler's murine encephalomyelitis virus-induced demyelinating disease (TMEV-IDD) and relapsing-remitting experimental autoimmune encephalomyelitis (R-EAE) in the SJL/J mouse are both relevant murine $CD4^+$ T cell-mediated demyelinating models that recapitulate the multiple sclerosis disease phenotypes. To determine the cellular and molecular basis for these observed differences in clinical course, we quantitatively analyzed the temporal expression of pro- and antiinflammatory cytokine mRNA expression in the central nervous system (CNS) and the phenotype of the inflammatory mononuclear infiltrates. TMEV-infected SJL/J mice expressed IFN-γ, TNF-α, IL-10, and IL-4 mRNA during the preclinical phase, and their levels continued to increase throughout the duration of the chronic-progressive disease course. These data correlated with the continued presence of both $CD4^+$ T cells and $F4/80^+$ macrophages within the CNS infiltrates. In contrast, SJL/J mice with $PLP_{139-151}$-induced R-EAE displayed a biphasic pattern of CNS expression for the proinflammatory cytokines, IFN-γ and TNF-α, with expression peaking at the height of the acute phase and relapse(s). This pattern correlated with dynamic changes in the $CD4^+$ T cell and $F4/80^+$ macrophage populations during relapsing-remitting disease progression. Interestingly, IL-4 message was undetectable until disease remission(s), demonstrating its potential role in the intrinsic regulation of ongoing disease, whereas IL-10 was continuously expressed, arguing against a regulatory role in either disease. These data suggest that the kinetics of cytokine expression together with the nature of the persistent inflammatory infiltrates are major contributors to the differences in clinical course between TMEV-IDD and R-EAE. ***The Journal of Immunology*****, 1998, 161: 4437–4446.**

Theiler's murine encephalomyelitis virus-induced demyelinating disease (TMEV-IDD)[3] and relapsing/remitting experimental autoimmune encephalomyelitis (R-EAE) are two well-characterized $CD4^+$ T cell-mediated models of multiple sclerosis (1, 2). Both diseases are characterized by an inflammatory mononuclear cell infiltrate within the central nervous system (CNS), resulting in demyelination and a subsequent ascending paralysis; however, each disease has a distinct clinical course in SJL/J mice (3, 4). Intracerebral infection of the susceptible SJL/J mouse with the BeAn strain of TMEV results in a chronic-progressive demyelinating disease, with the onset of clinical signs approximately 30 to 35 days postinfection (PI) (3, 5). In contrast, R-EAE induced by active immunization with the immunodominant epitope of PLP, $PLP_{139-151}$ (6), is characterized by an initial acute phase, followed by a series of remissions and relapses (7).

Despite the differences in the clinical course of these diseases, recent evidence suggests that the underlying immunopathologic mechanisms in these two models are similar. We have reported previously that in active $PLP_{139-151}$-induced R-EAE, the acute disease episode is mediated by T cells specific for the disease-initiating $PLP_{139-151}$ epitope, whereas the first clinical relapse is associated with reactivity to the non-cross-reacting $PLP_{178-191}$ epitope, a process termed epitope spreading (8, 9). Recent data indicate that epitope spreading may also contribute to the chronic nature of TMEV-IDD. Available evidence indicates that myelin damage is initiated by TMEV-specific $CD4^+$ T cells targeting CNS-persistent virus Ag, while the chronic stage of the disease involves $CD4^+$ myelin epitope-specific T cells primed via epitope spreading (10).

It is well documented that $CD4^+$ Th1 cells and their proinflammatory cytokines are suspected to be important in the pathogenesis of multiple sclerosis (11), and necessary for the induction of both TMEV-IDD (12–17) and R-EAE (7, 18, 19). In contrast to the inductive phase, there is conflicting information regarding the ongoing disease process and its regulation in both models. In R-EAE, cytokines such as IL-4, IL-10, and TGF-β have been implicated in disease resolution; however, these data are conflicting (20–22). In the present study, we therefore sought to characterize the nature of the persistent cellular infiltrate within the CNS in both TMEV-IDD and R-EAE and attempt to correlate it with the temporal changes in the pattern of cytokine expression and disease progression.

Using competitive quantitative PCR (CQ-PCR), we show that during TMEV-IDD, the mRNA for IFN-γ, TNF-α, IL-10, and IL-4 were first detectable before or coinciding with the onset of clinical signs. These data correlated with immunohistochemical evidence

Department of Microbiology-Immunology and Interdepartmental Immunobiology Center, Northwestern University Medical School, Chicago, IL 60611

Received for publication May 14, 1998. Accepted for publication June 12, 1998.

The costs of publication of this article were defrayed in part by the payment of page charges. This article must therefore be hereby marked *advertisement* in accordance with 18 U.S.C. Section 1734 solely to indicate this fact.

[1] This work was supported by U.S. Public Health Service National Institutes of Health Grants NS-26543, NS-30871, and NS-23349.

[2] Address correspondence and reprint requests to Dr. Stephen D. Miller, Department of Microbiology-Immunology, Northwestern University Medical School, 303 E. Chicago Avenue, Chicago, IL 60611. E-mail address: s-d-miller@nwu.edu

[3] Abbreviations used in this paper: TMEV-IDD, Theiler's murine encephalomyelitis virus-induced demyelinating disease; CNS, central nervous system; CQ-PCR, competitive quantitative PCR; EAE, experimental autoimmune encephalomyelitis; HPRT, hypoxanthine phosphoribosyltransferase; MCP, monocyte-chemotactic protein; MIP, macrophage-inflammatory protein; NOD, nonobese diabetic; PI, postinfection; PLP, proteolipid protein; R-EAE, relapsing EAE.

 0022-1767/98/$02.00

from spinal cord sections that indicated both persistent macrophage and T cell infiltrates as disease and demyelination progressed. The cytokine profile and the nature of cellular infiltrate were markedly different during the clinical course of R-EAE, wherein the maximal expression of the proinflammatory cytokines IFN-γ and TNF-α correlated with the clinical peaks of the acute phase and relapse(s). Unexpectedly, we did not find an association of IL-10 with remission, as was previously described (21), but rather found an increase in IL-4 message that was only detectable in mice recovering from the acute phase/relapse or those in complete remission. Most interestingly, these observed differences in cytokine expression correlated with dramatic changes in both the $CD4^+$ T cell and $F4/80^+$ macrophage populations within the CNS. Collectively, these data indicate that the combination of the cellular infiltrate and temporal cytokine expression within the CNS is largely responsible for the observed differences in clinical course of TMEV-IDD and R-EAE.

Materials and Methods

Mice

Female SJL/J mice, 6 to 7 wk old, were purchased from Harlan Laboratories (Indianapolis, IN). All mice were housed in the Northwestern animal care facility (Chicago, IL) and maintained on standard laboratory chow and water ad libitum. Severely paralyzed mice were afforded easier access to food and water.

Peptides

$PLP_{139-151}$ (HSLGKWLGHPDKF) was purchased from Peptide Synthesis Core Laboratories (University of North Carolina, Chapel Hill). Amino acid composition was verified by laser desorption mass spectroscopy, and purity (>98%) was assessed by HPLC.

Induction and clinical evaluation of R-EAE

Mice were immunized with 40 μg $PLP_{139-151}$ in CFA. Clinical severity was assessed daily and assigned a numerical grade of 0 to 5, as previously described (7). The data are plotted as the mean clinical score for each group of animals at the time of sacrifice. Each group of animals displayed clinical signs representative of the entire population.

Induction and clinical evaluation of TMEV-IDD

Mice were anesthetized with methoxyflurane (Mallinckrodt Veterinary, Mundelein, IL) and inoculated in the right cerebral hemisphere with 2.9×10^6 plaque-forming units of TMEV, strain BeAn 8386, in 30 μl DMEM. Mice were examined two to three times per week for the development of chronic gait abnormalities and spastic paralysis indicative of demyelination, and assigned a clinical score of 0 to 6, as follows: 0, asymptomatic; 1, mild waddling gait; 2, severe waddling gait, intact righting reflex; 3, severe waddling gait, spastic hind limb paralysis, impaired righting reflex; 4, severe waddling gait, spastic hind limb paralysis, impaired righting reflex, mild dehydration and/or malnutrition; 5, total hind limb paralysis, severe dehydration and/or malnutrition; and 6, death. The data are plotted as the mean clinical score for each group of animals at the time of sacrifice. Each group of animals displayed clinical signs representative of the entire population.

Isolation of RNA

At varying time points following induction of R-EAE or TMEV-IDD, mice (two per time point) were anesthetized and perfused through the left ventricle with 50 ml of PBS. Spinal cords were extruded by flushing the vertebral canal with PBS and then rinsed in PBS. Tissues were forced through a 100-mesh stainless steel screen to give a single cell suspension and pelleted by centrifugation ($500 \times g$) for 5 min at 4°C. The pellets were resuspended vigorously in 16 ml 4 M guanidinium isothiocyanate/50 mM Tris-Cl (pH 7.5)/25 mM EDTA (Life Technologies, Gaithersburg, MD), and 1% 2-ME and 0.5% *N*-lauroylsarcosine (Sigma-Aldrich, St. Louis, MO). Shearing of DNA was facilitated by forcing the resulting suspension repeatedly through a 23-gauge needle. Total RNA was isolated by high-speed gradient centrifugation (27,000 rpm) of 8 ml lysate through a 3 ml 5.7 M CsCl pad using a SW41 swinging bucket rotor for 20 h at 4°C. The resulting RNA pellet was resuspended to a final concentration of 1 μg/μl with diethylpyrocarbonate-treated water and stored in aliquots at −70°C.

First strand cDNA synthesis

First strand cDNA was generated from 2 μg total RNA using Advantage-RT Kit (Clontech, Palo Alto, CA) using 20 pmol oligo(dT) primer, per the manufacturer's provided protocol, in a total volume of 20 μl. Following first strand synthesis, each cDNA sample was brought to a final volume of 100 μl with distilled water.

CQ-PCR and densitometry

The PCR for all cytokines was performed with a previously described cytokine polycompetitor plasmid (pLOC) (23). The amount of pLOC, cDNA, and final $MgCl_2$ concentration was determined empirically for each cytokine tested. Additions of pLOC ranged from 10 μl of a 0.5 ng/ml stock (IL-4) to 10 μl of a 250 ng/ml stock (hypoxanthine phosphoribosyltransferase; HPRT) per each 50-μl PCR reaction. Final PCR conditions included 50 mM KCl, 10 mM Tris-Cl (pH 8.3), 2.5 to 5 mM $MgCl_2$, 2 mM dNTPs, 100 pmols of each 5′ and 3′ gene-specific primer, 1 U *Taq* polymerase (Qiagen, Chatsworth, CA), and 5 to 10 μl diluted cDNA. The primers were synthesized by Life Technologies, and amplify both the competitor plasmid and wild-type cDNA. Cycling conditions were 94°C, 40 s; 60°C, 20 s; and 72°C, 40 s, for a total of 30 cycles, linked to a final 72°C extension program for 3 min and then to a final 4°C soak program. PCR products were run on an ethidium bromide-containing 2% agarose gel and illuminated using a UV light source, then photographed using Polaroid type 667 film. Gel images were then scanned into Adobe Photoshop using an Epson ES 1200-C scanner and imported as TIFF files into Kodak 1D Digital Science for densitometry. The sum intensity and band area were determined for each competitor/wild-type amplicon pair, and a ratio of wild-type/competitor intensity was determined for all cytokines and adjusted to each sample's housekeeping gene, HPRT. Sum intensity values for each wild-type amplicon were also adjusted for the difference in size to that of the competitor band to account for increased ethidium bromide incorporation in the higher m.w. competitor band. Attomoles of target cDNA were determined by multiplying the adjusted wild-type/competitor ratio with the amount of pLOC added to each sample and then adjusted for the amount of cDNA used in each PCR amplification.

Immunohistochemistry and quantitation of $CD4^+$ and $F4/80^+$ cells

For immunohistochemistry, two mice per time point were perfused with PBS, as described in a previous *Materials and Methods* section. Spinal cords were dissected out and flash frozen in O.C.T. compound (Fisher, Itasca, IL). Random 6-μm sections from the lumbar region of the spinal cord were cut and fixed in acetone. For CD4 staining, slides were incubated with biotinylated anti-L3T4 (PharMingen, San Diego, CA), and for macrophage staining, with biotinylated anti-F4/80 (Caltag, San Francisco, CA), for 1 h at room temperature. All slides were then rinsed and processed through a secondary incubation with avidin-biotin-peroxidase complex (Vector Labs, Burlingame, CA). Color was developed using diaminobenzidine (DAB; Kirkegaard & Perry Laboratories, Gaithersburg, MD), counterstained using contrast green, dehydrated, and mounted in Accu-Mount-60 (Stephens Scientific, Riverdale, NJ). Following CD4 and F4/80 immunohistochemistry, for each time point, eight serial lumbar sections were analyzed using a grid reticle viewfinder at ×100 magnification. At this magnification, each grid measures a 9-mm^2 area, and represents approximately 5 to 7% of the total white matter. A total of twelve 9-mm^2 areas was measured per cord representing an equal distribution between ventral, dorsal, and both lateral regions. Gray matter was not analyzed because neither R-EAE nor TMEV-IDD typically present with infiltration into this region of the CNS. Data are presented in tabular form as the mean number of positive cells ± the SEM for the entire 27-mm^2 ventral, dorsal, and lateral regions analyzed.

Results

TMEV-IDD and R-EAE display distinct clinical disease patterns in SJL mice

SJL mice were monitored for the development of clinical signs of demyelination following infection with TMEV and following priming with $PLP_{139-151}$/CFA (Fig. 1). Clinical signs in R-EAE were first evident on day 13 postimmunization, and disease symptoms rapidly increased, peaking on day 14. Characteristic of R-EAE, this acute phase was followed by a remission that lasted through day 19 and the subsequent reappearance of a clinical relapse that peaked approximately day 26 postimmunization

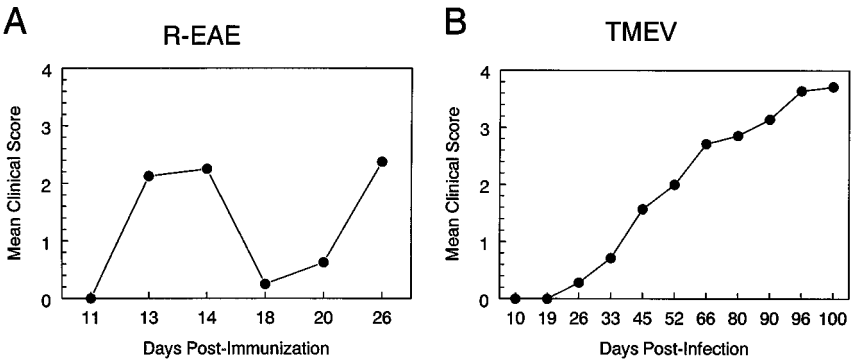

FIGURE 1. Comparison of clinical disease course between SJL mice with $PLP_{139-151}$-induced R-EAE and TMEV-IDD. R-EAE (*A*) and TMEV-IDD (*B*) were induced in SJL/J mice, and all animals were graded for clinical signs, as described in *Materials and Methods*. Results are expressed as mean clinical score of affected animals at the point of sacrifice versus days postimmunization/infection. Clinical scores depicted are representative of all animals in each group, and disease incidence in both groups was 100%.

(Fig. 1*A*). In contrast to R-EAE, the clinical progression of TMEV-IDD proceeded along a much slower path. The initial clinical impairment of a mild waddling gait was not apparent until approximately 33 days PI in TMEV-infected animals. Clinical signs then persisted in a chronic nature of an ascending and spastic hind limb paralysis until the termination of the experiment at 100 days PI (Fig. 1*B*).

Temporal immunohistochemical analysis of CNS mononuclear infiltrates in TMEV-IDD and R-EAE

To better understand the observed differences in clinical course between these two disease models, we quantitated the phenotypic nature and localization of the CNS mononuclear infiltrates in situ at varying times during the course of disease using immunohistochemistry. Previous studies have demonstrated that $CD4^+$ T cells are necessary for the induction of both TMEV-IDD (14, 15, 24) and R-EAE (7, 19) in SJL mice. Our analysis was therefore aimed at determining not only the nature and location of the initial infiltrate at disease onset, but also its dynamics as disease progressed.

During the course of R-EAE, the $CD4^+$ T cell and $F4/80^+$ macrophage infiltrate displayed very dramatic changes. The $CD4^+$ population was scarcely detectable (0.73–2.19 positive cells/spinal cord region) during the preclinical phase at 5 to 6 days postimmunization (Fig. 2*A*), but increased by approximately 20-fold in all analyzed areas of white matter at the peak of the acute phase of disease 3 days thereafter (Fig. 2*B* and Table I). This increase in the number of $CD4^+$ cells correlated with the rapid onset of clinical disease (Fig. 1*A*). As the mice progressed into a spontaneous full remission approximately 18 days postimmunization, the $CD4^+$ T cell levels decreased dramatically to levels (1.21–5.86 positive cells/region) only slightly greater than those seen during the preclinical phase (Fig. 2*C*), but then dramatically increased (18.67–41.83 positive cells/section) as the mice began to clinically relapse (Fig. 2*D*). It is interesting to note that as the clinical scores began to decline as the mice entered remission (remitting), the number of $CD4^+$ cells had already decreased significantly, despite maintaining a clinical score of at least 1 (Table I). In addition, the amount and pattern of the infiltrate were similar in both the acute phase and the relapse, and were detectable to the same degree in all spinal cord regions (ventral, lateral, and dorsal) analyzed, indicating a widespread targeting of myelin destruction. The $F4/80^+$ macrophage population progressed in a similar biphasic manner as compared with the $CD4^+$ T cells, peaking at the height of the acute and relapsing clinical episodes. However, the relative numbers of $F4/80^+$ cells were two- to threefold increased over the numbers of $CD4^+$ T cells during both the acute phase and the relapse (Fig. 3, *A–D*, and Table I). The localization of the $F4/80^+$ macrophages in the CNS lesions generally overlapped with the $CD4^+$ T cells. However, one unexpected observation was that during the first relapse there were significantly more $F4/80^+$ cells detected than during the acute phase. The significance of this observation may relate to the onset of epitope spreading of $CD4^+$ T cell responses to endogenous myelin epitopes and the subsequent induction of additional relapses.

Temporal immunohistochemical analysis of the expression of $CD4^+$ and $F4/80^+$ cells in the spinal cords of TMEV-infected animals revealed a remarkably different pattern. At day 49 PI, approximately 2 wk following the onset of clinical signs, high numbers of both $CD4^+$ T cells and $F4/80^+$ macrophages/microglia were observed in the spinal cord infiltrates (Figs. 2*E* and 3*E* and Table II). The numbers of $CD4^+$ T cells and $F4/80^+$ macrophages increased by twofold by day 79 PI, and correlate with a corresponding increase in disease severity (Fig. 1*B*). As disease progressed to day 104 PI, the numbers of $CD4^+$ T cells and $F4/80^+$ macrophages remained elevated, but had decreased slightly, most likely as a result of dehydration due to severe paralysis. In contrast to R-EAE, the localization of the infiltrate was not as widespread, but rather restricted primarily to the ventral spinal cord region as the infiltrates persisted at higher levels in this region. An increase in $CD4^+$ and $F4/80^+$ cells was, however, detected in all sections at various times during early disease progression. The significance of this finding is not apparent, but may be related to the progression of a natural viral-induced demyelinating disease, wherein virus persists in CNS-resident macrophages/microglia versus an experimentally induced demyelinating model as in R-EAE.

Similar patterns in the number of infiltrating $CD4^+$ and $F4/80^+$ cells in R-EAE and TMEV-IDD at various stages of the disease course, as determined by the immunohistochemical analysis above, were confirmed by a flow-cytometric analysis of CNS mononuclear cells isolated from the spinal cords of affected mice on discontinuous Percoll gradients (data not shown). Additionally, although $CD8^+$ T cell infiltrates were detectable in both R-EAE and TMEV-IDD and their temporal changes in number mimicked that of the $CD4^+$ T cell population, their percentages were significantly lower and their fluctuations were not as dramatic. Similarly, the temporal changes in the $B220^+$ population were not as striking as those seen with the $CD4^+$ and macrophage populations, as their total percentage never exceeded 2 to 5% of the total infiltrate in either model.

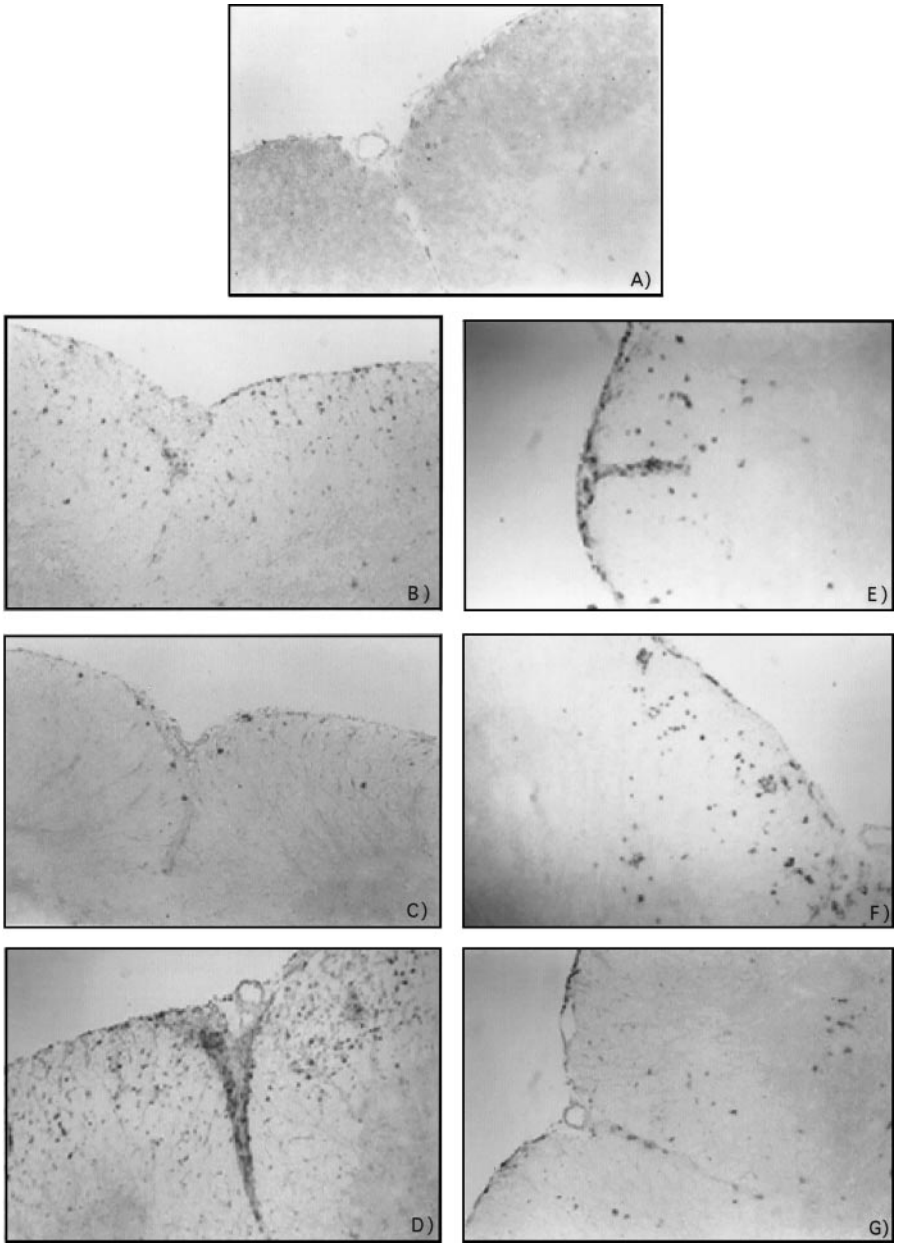

FIGURE 2. Immunohistochemical staining for $CD4^+$ T cells in the spinal cords of SJL mice with $PLP_{139-151}$-induced R-EAE and TMEV-IDD. Spinal cord sections from mice at various times after the induction of R-EAE (*A*, preclinical; *B*, peak of acute episode; *C*, remission; *D*, peak of primary relapse) and after TMEV infection (*E*, day 49; *F*, day 79; *G*, day 104) were stained for expression of CD4 using anti-L3T4 and counterstained with contrast green. Magnification is ×100. Isotype-matched control Ab did not stain spinal cords from affected mice (data not shown).

Temporal analysis of Th1-dependent proinflammatory cytokine mRNA in TMEV-IDD and R-EAE by CQ-PCR

The data to this point indicate that the clinical presentation and the temporal changes in the inflammatory infiltrates in TMEV-IDD and R-EAE differ dramatically, despite the presence of similar immune populations in roughly the same ratios. We next sought to determine whether the pattern of proinflammatory cytokine expression in the target organ of the CNS would provide additional insight into the differences between these two demyelinating models. Total RNA was isolated from the spinal cords of SJL mice at varying times after induction of R-EAE or TMEV-IDD, and subjected to CQ-PCR to determine message levels for the proinflammatory cytokines IFN-γ and TNF-α. Figure 4*A* shows a representative ethidium bromide-stained agarose gel profile of the CQ-PCR for IFN-γ, and TNF-α for both R-EAE and TMEV-IDD. In CQ-PCR, the larger amplicon is that of the competitor, while the lower band is that specifically amplified from target cDNA. The concentration of competitor that was used was empirically determined and was different for each cytokine examined. Densitometry analysis of the resulting amplified products from IFN-γ and TNF-α CQ-PCR yielded the quantitative data shown in Figure 5 for spinal cord mRNA levels for mice undergoing both R-EAE and TMEV-IDD.

During the relapsing course of R-EAE, IFN-γ and TNF-α mRNA displayed a biphasic pattern of expression, with increased levels coinciding with increasing incidence of clinical severity at the day of onset of initial clinical signs, and at the first relapse (Fig. 5*A*). Expression of IFN-γ and TNF-α was not detectable during the preclinical period (5 days postimmunization); however, the analysis of additional time points 1 to 2 days before the onset of clinical signs

Table I. *Quantitation of CD4$^+$ T cells and F4/80$^+$ macrophages/microglia from the spinal cords of SJL/J mice with PLP$_{139-151}$-induced R-EAE*

Cell Population[a]	Disease Stage	Spinal Cord Region		
		Ventral	Dorsal	Lateral
CD4	Preclinical	2.19 ± 0.48	1.13 ± 0.32	0.73 ± 0.21
	Acute	36.60 ± 1.59	19.94 ± 1.75	24.03 ± 1.91
	Remitting	5.13 ± 0.95	3.80 ± 1.04	12.29 ± 2.13
	Remission	5.86 ± 1.65	1.29 ± 0.30	1.21 ± 0.29[b]
	Relapse	38.77 ± 5.22	18.67 ± 2.25	34.28 ± 2.70[c]
F4/80	Preclinical	0.88 ± 0.22	0.19 ± 0.10	0.06 ± 0.04
	Acute	52.43 ± 5.62	38.35 ± 2.72	44.76 ± 3.81
	Remitting	7.00 ± 0.99	1.56 ± 0.65	0.66 ± 0.27
	Remission	4.50 ± 1.19	1.25 ± 0.44	3.56 ± 0.99
	Relapse	118.31 ± 15.93[c]	80.38 ± 14.39[c]	128.26 ± 15.62[c]

[a] The numbers of CD4$^+$ T cells and F4/80$^+$ macrophages/microglia were quantitated from the spinal cords of SJL/J mice at various stages of R-EAE (two mice per time point) as detailed in *Materials and Methods.* Data are shown as the mean number of positive cells per each 27-mm^2 ventral, dorsal, and lateral area ± SEM.
[b] No significant difference from preclinical value; all other values are significantly greater than preclinical levels ($p < 0.05$).
[c] Relapse values significantly greater than those at the peak of acute disease ($p < 0.05$).

revealed detectable levels of both proinflammatory cytokines, despite the fact that the animals were still asymptomatic (data not shown). In contrast, IFN-γ expression from TMEV-IDD-affected mice was first detectable as early as day 14 PI, several weeks before the onset of overt clinical signs (Fig. 5*B*). TNF-α expression lagged slightly behind, being first detectable at day 33 PI, approximately coincident with the day of clinical disease onset. Once induced, the levels of both cytokines continued to increase throughout the chronic phase of disease (last time point examined, day 103 PI). Similar to IFN-γ and TNF-α, the expression pattern of lymphotoxin-α paralleled the increases in disease severity during both R-EAE and TMEV-IDD (data not shown). Overall, the profile for the proinflammatory IFN-γ and TNF-α again correlated with the nature of the infiltrate and clinical course, being biphasic in R-EAE and chronic-progressive in TMEV-IDD.

Temporal analysis of Th2-dependent antiinflammatory cytokine mRNA expression in TMEV-IDD and R-EAE by CQ-PCR

Recent evidence suggests that the Th2 cytokines, IL-4 and/or IL-10, may be involved in down-regulation of ongoing R-EAE (21, 22, 25, 26). Employing CQ-PCR, we determined the expression pattern of IL-4 and IL-10 mRNA in the CNS during both R-EAE and chronic TMEV-IDD. Representative ethidium bromide-stained agarose gel profiles for both cytokines are shown in Figure 4*B.* Similar to the expression pattern of the proinflammatory cytokines during TMEV-IDD, CQ-PCR analysis revealed that both IL-4 and IL-10 were detectable before the onset of clinical signs, 14 to 26 days PI, and their expression continued throughout the chronic-progressive disease course (Fig. 6*B*). Overall, in both models, the amount of detectable Th2-derived cytokine mRNA was approximately 10-fold lower than that observed for the proinflammatory cytokines. Given this data, it would appear that in the TMEV model, the early and prolonged expression of Th2 cytokines within the CNS is unable to down-regulate the Th1 response thought to be responsible for demyelination and clinical disease.

The pattern of mRNA expression of IL-10 and IL-4 during R-EAE was perhaps the most interesting (Fig. 6*A*). In contrast to a previous report (21) using semiquantitative RT-PCR suggesting that IL-10 may be involved in mediating disease remission in the SJL mouse, our data indicate that IL-10 expression does not correlate with the onset of remission. As in TMEV-IDD, IL-10 was detectable at the time of disease onset and remained elevated through the first remission and subsequent relapse. In contrast, IL-4 expression was only detectable in animals remitting from the acute clinical episode or in full remission from acute disease, suggesting that expression of this cytokine may be an important intrinsic mechanism involved in mediating disease remission.

Previous reports have not quantitated the expression of the Th2 cytokines in the CNS of mice with R-EAE beyond the first remission. Given our interesting observations on the potential regulatory role of IL-4, we wanted to determine whether pro- and antiinflammatory cytokine mRNA expression in the CNS or mice with R-EAE would continue to flux as the animals progressed further in the disease course. Therefore, we performed another R-EAE time course and followed animals through the first relapse into a second remission and a subsequent second relapse. Once again, the pattern of IL-10 expression did not increase or decrease relative to the disease state, whereas IL-4 was strictly correlated with disease remission (Fig. 7), and expression of IFN-γ and TNF-α correlated with increases in clinical severity during the acute phase and first and second relapses (not shown).

Discussion

In the present study, we quantitatively analyzed the temporal expression of pro- and antiinflammatory cytokine mRNA expression in the CNS and assessed the number and anatomic location of CD4$^+$ T cell and F4/80$^+$ macrophage/microglia within CNS inflammatory infiltrates of mice undergoing both R-EAE and TMEV-IDD. The different clinical disease patterns of the R-EAE and chronic-progressive TMEV-IDD suggested distinct underlying mechanisms; however, the data revealed both striking similarities and differences between the two models.

Immunohistochemical staining and quantitation of absolute cell numbers from the spinal cords of affected mice revealed that, for both models, the majority of the CNS cellular infiltrate was comprised of CD4$^+$ T cells and F4/80$^+$ macrophages. Interestingly, the increases in both of these populations correlated directly with increasing disease severity in R-EAE and TMEV-IDD. These data related to the CD4$^+$ T cells are not surprising given previous reports of their essential role in the induction of both R-EAE (7, 19) and TMEV-IDD (14, 15). Our observations, however, further elaborate on the role of CD4$^+$ T cells. The increased numbers of CD4$^+$ T cells at the peak of acute phase and at the height of the first clinical relapse during R-EAE, as well as their continued presence throughout the chronic phase of TMEV-IDD, implicate them not only in disease induction, but also more importantly, in disease progression. This observation is supported by recent data from our lab demonstrating that PLP$_{139-151}$, and subsequently PLP$_{178-191}$-specific T cells, are responsible for mediating the initial acute phase and first clinical relapse of R-EAE, respectively, a

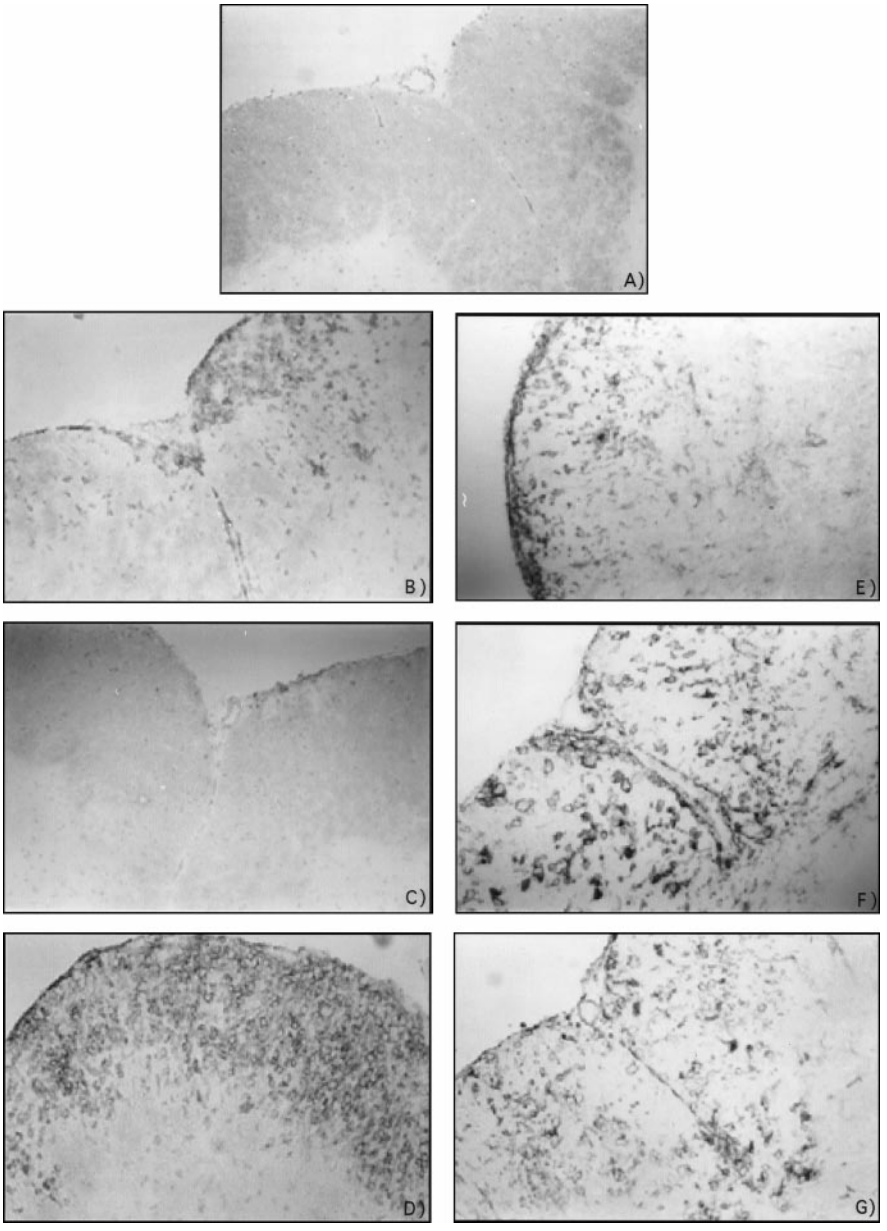

FIGURE 3. Immunohistochemical staining for F4/80$^+$ macrophages/microglia in the spinal cords of SJL mice with $PLP_{139-151}$-induced R-EAE and TMEV-IDD. Spinal cord sections from mice at various times after the induction of R-EAE (*A*, preclinical; *B*, peak of acute episode; *C*, remission; *D*, peak of primary relapse) and after TMEV infection (*E*, day 49; *F*, day 79; *G*, day 104) were stained for expression of F4/80 using biotinylated anti-F4/80 and counterstained with contrast green. Magnification is ×100. Isotype-matched control Ab did not stain spinal cords from affected mice (data not shown).

phenomenon termed epitope spreading (8, 27). In addition, we and others have also previously demonstrated the importance of virus-specific CD4$^+$ T cells in initiating myelin damage by targeting CNS-persistent virus in TMEV-infected SJL/J mice (12, 13, 15–17, 28, 29). In contrast, the chronic stage of TMEV-IDD also involves pathologic damage mediated by myelin epitope-specific CD4$^+$ T cells that first

Table II. *Quantitation of CD4$^+$ T cells and F4/80$^+$ macrophages/microglia from the spinal cords of SJL/J mice with TMEV-IDD*

		Spinal Cord Region		
Cell Population[a]	Day p.i.	Ventral	Dorsal	Lateral
CD4	49	25.88 ± 3.57	1.13 ± 0.55[b]	31.94 ± 8.24
	79	57.50 ± 5.50	44.25 ± 6.58	31.81 ± 5.95
	104	30.38 ± 3.46	5.57 ± 1.53	9.13 ± 1.33
F4/80	49	20.63 ± 2.59	2.00 ± 0.68	42.19 ± 10.18
	79	121.75 ± 6.49	78.88 ± 8.61	90.00 ± 5.61
	104	102.50 ± 3.88	37.75 ± 16.39	31.38 ± 8.20

[a] The numbers of CD4$^+$ T cells and F4/80$^+$ macrophages/microglia were quantitated from the spinal cords of SJL/J mice at various days p.i. with TMEV (two mice per time point) as detailed in *Materials and Methods*. Data are shown as the mean number of positive cells per each 27-mm^2 ventral, dorsal, and lateral area ± SEM.

[b] No significant difference from preclinical values shown in Table I; all other values are significantly greater than preclinical levels ($p < 0.05$).

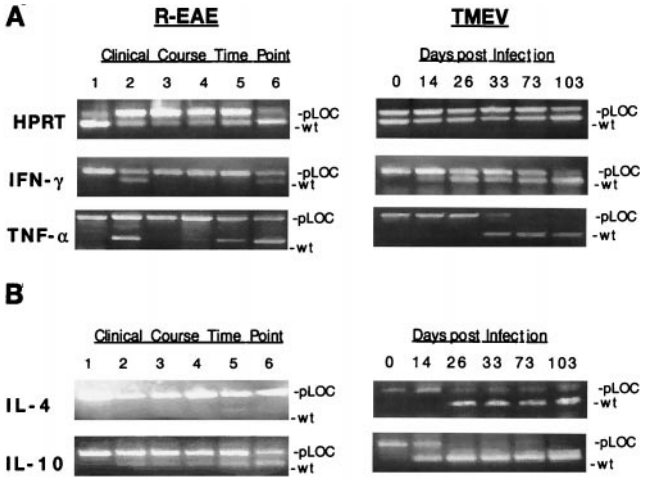

FIGURE 4. Representative time course profile of CQ-PCR for HPRT, IFN-γ, TNF-α, IL-4, and IL-10 from the spinal cords of SJL mice with $PLP_{139-151}$-induced R-EAE and TMEV-IDD. RNA was isolated from pooled spinal cords (at least two mice per time point) of mice at varying times after the induction of R-EAE and TMEV-IDD. CQ-PCR samples were prepared as described in *Materials and Methods*. Data shown are scanned images of ethidium bromide-stained 2% agarose gels. The higher m.w. band represents the polycompetitor plasmid (pLOC) DNA, while the lower band is amplified from wild-type sample cDNA. For TMEV-IDD, days PI are noted. The lane numbers for mice with R-EAE correspond to *1*, preclinical; *2*, day of onset; *3*, peak of acute phase; *4*, remitting; *5*, remission; and *6*, first relapse. Clinical scores for animals at each time point are shown in Figure 1.

arise 2 to 3 wk after the onset of clinical signs of disease via epitope spreading (10).

As stated previously, we also observed that increases in the F4/80^+ macrophage population correlated with increasing disease severity and with periods of expression of high levels of TNF-α mRNA in the CNS. These results are consistent with previous histologic evidence showing that activated macrophages/microglia play a major role in myelin destruction in both disease models (30), and that TNF-α expression is a sensitive marker for activated macrophages (31). Interestingly, we also observed that the numbers of macrophages increased to two- to threefold the number of $CD4^+$ T cells as clinical disease progressed during both R-EAE and TMEV-IDD. This result is interesting and may point to a pivotal role of this population in the perpetuation of epitope spreading and the resulting chronic demyelination. In this regard, we have demonstrated recently that F4/80^+, I-A^{s+} macrophages/microglia isolated from the spinal cords of mice 90 days PI with TMEV express high levels of B7 costimulatory molecules (56), and endogenously activate both virus-specific and myelin epitope-specific Th1 cells in vitro in the absence of exogenously added Ag (unpublished observation). Facilitation of epitope spreading by activated macrophages may occur through continuing active phagocytosis of myelin debris and subsequent processing and presentation of self epitopes within CNS lesions, as well as by the production of chemokines (e.g., MIP-1α and MCP-1), leading to the recruitment of additional peripheral macrophages and T cells (32, 33), and the production of proinflammatory cytokines (e.g., TNF-α, IFN-γ, and IL-12) active in the recruitment (34) and/or local activation (35) of myelin epitope-specific Th1 cells.

Currently, there is no cell surface molecule that can distinguish between infiltrating peripheral macrophages and CNS resident microglia. Therefore, it is possible that our quantitation of F4/80^+ cell numbers includes activated microglia as an additional correlate of disease progression. Additionally, this pattern of increased macrophages in the first relapse of R-EAE versus the acute phase correlates well with published observations related to chemokine production in R-EAE in the SJL mouse. We have shown that CNS expression of MIP-1α correlated with acute disease development (32, 33), whereas expression of MCP-1 did not. In contrast, MCP-1 production in the CNS correlated with relapsing EAE development (33). Moreover, anti-MIP-1α, but not anti-MCP-1, inhibited development of acute but not relapsing EAE, whereas anti-MCP-1 significantly reduced the severity of relapsing EAE. This expression pattern is consistent for a predominant role for MIP-1α in inducing T cell infiltration into the CNS during disease initiation and a more predominant role for MCP-1 in directing macrophage infiltration during relapses.

Interestingly, in both models, the increases in the $CD4^+$ population also paralleled increases in mRNA for both IFN-γ and TNF-α. These data correlate well with that of others who have demonstrated previously the integral role of Th1 cells and proinflammatory cytokines during disease initiation for R-EAE and TMEV-IDD (18, 36–39). Our data extend the role of the proinflammatory cytokines by demonstrating their importance in the perpetuation of ongoing disease. Additionally, the message for TNF-α exceeded that for IFN-γ in both models and supports our

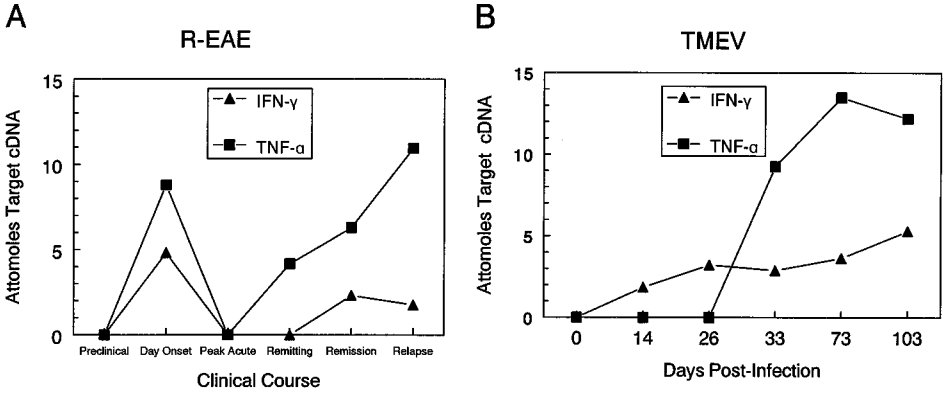

FIGURE 5. Competitive PCR quantitation of the temporal course of proinflammatory cytokine mRNA expression in the spinal cords of SJL mice with $PLP_{139-151}$-induced R-EAE (*A*) and TMEV-IDD (*B*). Spinal cord RNA (2 μg) was isolated from affected mice and used as a template in CQ-PCR, as described. Clinical scores for animals at each time point are shown in Figure 1. Each IFN-γ PCR reaction contained 10 μl 25 ng/ml pLOC and 5 μl wild-type template, and each TNF-α PCR reaction contained 10 μl 50 ng/ml pLOC and 5 μl wild-type template. Ethidium bromide-stained images were scanned for densitometry (Kodak Digital 1D Science), and attomole amounts for each sample were calculated from obtained values, as described in *Materials and Methods*.

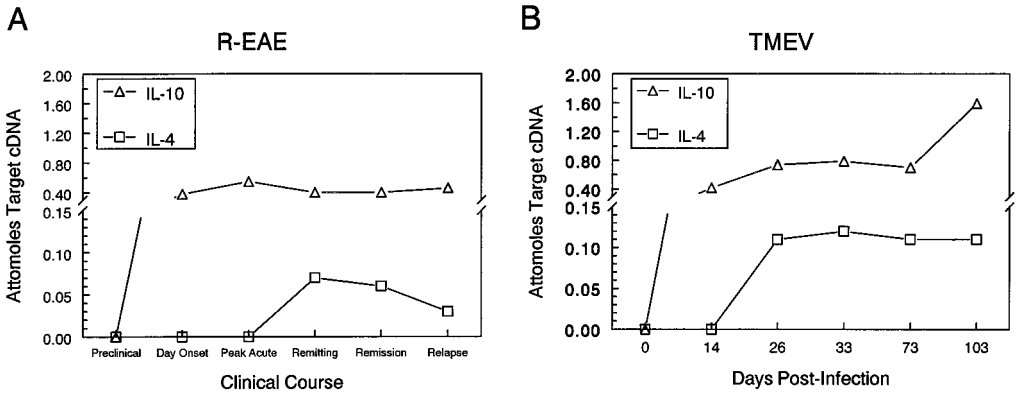

FIGURE 6. Competitive PCR quantitation of the temporal course of antiinflammatory cytokine mRNA expression in the spinal cords of SJL mice with $PLP_{139-151}$-induced R-EAE (*A*) and TMEV-IDD (*B*). Spinal cord RNA (2 μg) was isolated from affected mice and used as a template in CQ-PCR, as described. Clinical scores for animals at each time point are shown in Figure 1. Each IL-4 PCR reaction contained 10 μl 0.5 ng/ml pLOC and 10 μl wild-type template, and each IL-10 PCR reaction contained 10 μl 2.5 ng/ml pLOC and 10 μl wild-type template. Ethidium bromide-stained images were scanned for densitometry (Kodak Digital 1D Science), and attomole amounts for each sample were calculated from obtained values, as described in *Materials and Methods.*

observations related to the absolute cell numbers within the infiltrate. As discussed above, this proinflammatory cytokine is most likely being produced by the infiltrating $F4/80^+$ macrophages (31), but activated resident microglia and/or astrocytes within the CNS may also contribute to its production (40, 41). The resulting increase in the $F4/80^+$ population during the first relapse of R-EAE also correlates with the observed increase in TNF-α mRNA in comparison with levels achieved during acute disease. Interestingly, recent reports have indicated that IFN-γ (42, 43) and TNF-α (38, 44, 45) are not necessary for the induction of R-EAE, whereas the role of lymphotoxin-α is still in question (38). It is important to note that all of these studies utilized knockouts on the C57BL/6 background, a strain that is genetically resistant to EAE induction in the absence of treatment with pertussis toxin. Regardless, our results indicate that in the SJL/J mouse the temporal appearance of $CD4^+$ T cell and $F4/80^+$ macrophage populations, as well as the expression kinetics of the proinflammatory cytokines IFN-γ and TNF-α are excellent predictors of the progression of the clinical disease course of both R-EAE and TMEV-IDD.

In contrast to IFN-γ and TNF-α, the expression of the Th2 cytokines, IL-4 and IL-10, did not correlate with the peaks of clinical severity. Several previous studies have suggested a role for IL-10 in R-EAE remission (21, 46). In contrast, our results, which employed three separate time course experiments, indicated no such correlation, in that IL-10 mRNA was expressed preclinically and increased as disease progressed in both R-EAE and chronic-progressive TMEV-IDD. The reasons for this discrepancy are unclear, but may relate to the use of an myelin basic protein-adoptive transfer system to induce R-EAE in one study (21) and the use of mRNA from CNS inflammatory infiltrates in a Lewis rat EAE model in the other (46). We felt it necessary to analyze mRNA from the entire spinal cord since cytokines such as TNF-α and IL-10 can also be produced by resident CNS populations such as microglia and astrocytes, and could therefore contribute to the resulting R-EAE or TMEV-IDD pathology (40, 41). Our data are consistent with earlier reports in EAE demonstrating that administration of IL-10 failed to protect mice from the onset or progression of adoptive R-EAE (25) and in the NOD mouse, wherein expression of transgene IL-10 in pancreatic β cells actually accelerated development of diabetes (47). Current experiments employing immunohistochemistry and in situ PCR are underway to determine which cell population(s) within the CNS produces IL-10 during the course of autoimmune and virus-induced demyelination.

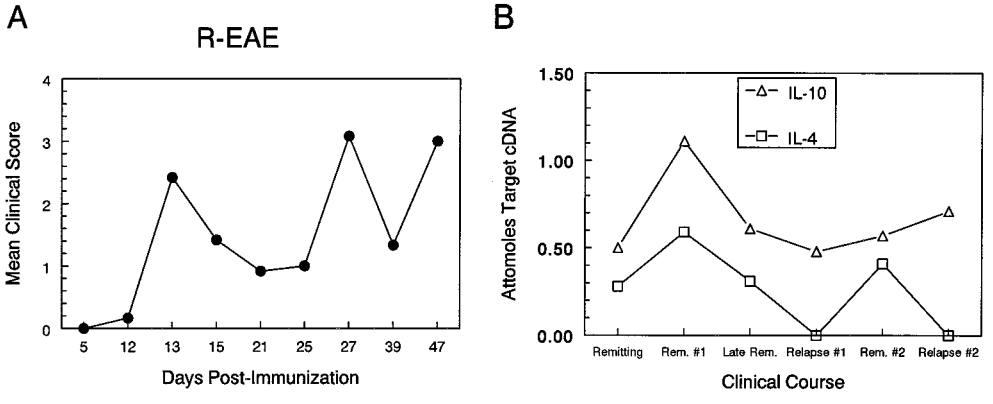

FIGURE 7. IL-4, but not IL-10, CNS mRNA expression correlates with the onset of remissions in R-EAE. R-EAE was induced in a large group of SJL mice by immunization with $PLP_{139-151}$/CFA, and affected animals were scored for clinical signs of demyelination through the second relapse, as previously described (*A*). Spinal cord RNA (2 μg) was isolated from affected mice and used as a template in CQ-PCR, as described previously (*B*). Each IL-4 PCR reaction contained 10 μl 0.5 ng/ml pLOC and 10 μl wild-type template, and each IL-10 PCR reaction contained 10 μl 2.5 ng/ml pLOC and 10 μl wild-type template. Ethidium bromide-stained images were scanned for densitometry (Kodak Digital 1D Science), and attomole amounts for each sample were calculated from obtained values, as described in *Materials and Methods.*

The correlation of peak IL-4 mRNA expression during the first and second remissions is perhaps our most intriguing finding and further supports recent evidence for a role of this cytokine in down-regulation of autoimmune diseases. IL-4 has been reported to regulate EAE in a number of experimental settings, including the natural recovery from disease in the Lewis rat (48), and as an important mediator following tolerance induction by either oral administration of Ag (49) or immunization with altered peptide ligands (50). More recently, it has been reported that specific targeting of IL-4-producing neuroantigen-specific T cell hybridomas to the CNS led to the amelioration of R-EAE (22). Using similar methodology, Mathisen et al. showed that neuroantigen-specific Th2 clones producing constitutive IL-4 and transgene IL-10 could decrease EAE severity (26). Further support for a potential down-regulatory role of IL-4 has come from NOD mouse, in which it has been shown recently that targeted expression of IL-4 within pancreatic β cells protected these normally susceptible NOD mice from the onset of both insulitis and diabetes (51).

Our findings showing the biphasic expression of IL-4 mRNA corresponding to disease remissions are the first demonstration that IL-4 may play an important role in mediating the intrinsic regulation in the $PLP_{139-151}$-induced R-EAE system. It is important to note, however, that in the SJL/J mouse, IL-4 mRNA expression within the spinal cord does not always coincide with a decrease in clinical severity. IL-4 expression in TMEV-IDD was detectable as early as 14 days PI, several weeks before the onset of clinical signs, and yet all TMEV-infected animals went onto develop a chronic-progressive demyelinating disease. A similar pattern of IL-4 mRNA expression has also been observed in SJL/J mice infected with the more virulent DA strain of TMEV (52). Given that TMEV persists in macrophages/microglia within the CNS of infected SJL mice (53–55), it is possible that a local environment is established that favors the continued activation of Th1 responses, e.g., up-regulated IL-12, etc., in spite of the presence of Th2 cytokines.

Collectively, our findings support an important role for $CD4^+$Th1 cells and $F4/80^+$ macrophages, as well as the associated proinflammatory cytokines IFN-γ and TNF-α as important mediators not only of disease induction, but also of disease progression during the distinct clinical courses of both R-EAE and chronic-progressive TMEV-IDD. Our data also suggest a significant role for IL-4, but not IL-10, in promoting R-EAE remission. Finally, our data indicate that examination of the cytokine profile in the target organ during the progression of autoimmune diseases may provide insights into not only the underlying immunopathologic mechanism(s), but also suggest possible therapeutic strategies aimed at complementing the immune system's intrinsic efforts to down-regulate the autoimmune pathology.

References

1. Miller, S. D., and S. J. Gerety. 1990. Immunologic aspects of Theiler's murine encephalomyelitis virus (TMEV)-induced demyelinating disease. *Semin. Virol. 1:263.*
2. Miller, S. D., and W. J. Karpus. 1994. The immunopathogenesis and regulation of T-cell mediated demyelinating diseases. *Immunol. Today 15:356.*
3. Lipton, H. L., and M. C. Dal Canto. 1979. Susceptibility of inbred mice to chronic central nervous system infection by Theiler's murine encephalomyelitis virus. *Infect. Immun. 26:369.*
4. Brown, A. M., and D. E. McFarlin. 1981. Relapsing experimental allergic encephalomyelitis in the SJL/J mouse. *Lab. Invest. 45:278.*
5. Lipton, H. L. 1980. Persistent Theiler's murine encephalomyelitis virus infection in mice depends on plaque size. *J. Gen. Virol. 46:169.*
6. Kennedy, M. K., L. J. Tan, M. C. Dal Canto, V. K. Tuohy, Z. J. Lu, J. L. Trotter, and S. D. Miller. 1990. Inhibition of murine relapsing experimental autoimmune encephalomyelitis by immune tolerance to proteolipid protein and its encephalitogenic peptides. *J. Immunol. 144:909.*
7. McRae, B. L., M. K. Kennedy, L. J. Tan, M. C. Dal Canto, and S. D. Miller. 1992. Induction of active and adoptive chronic-relapsing experimental autoimmune encephalomyelitis (EAE) using an encephalitogenic epitope of proteolipid protein. *J. Neuroimmunol. 38:229.*
8. McRae, B. L., C. L. Vanderlugt, M. C. Dal Canto, and S. D. Miller. 1995. Functional evidence for epitope spreading in the relapsing pathology of EAE in the SJL/J mouse. *J. Exp. Med. 182:75.*
9. Vanderlugt, C. L., and S. D. Miller. 1996. Epitope spreading. *Curr. Opin. Immunol. 8:831.*
10. Miller, S. D., C. L. Vanderlugt, W. S. Begolka, W. Pao, R. L. Yauch, K. L. Neville, Y. Katz-Levy, A. Carrizosa, and B. S. Kim. 1997. Persistent infection with Theiler's virus leads to CNS autoimmunity via epitope spreading. *Nat. Med. 3:1133.*
11. Beck, J., P. Rondot, L. Catinot, E. Falcoff, H. Kirchner, and J. Wietzerbin. 1988. Increased production of interferon γ and tumor necrosis factor precedes clinical manifestation in multiple sclerosis: do cytokines trigger off exacerbations? *Acta Neurol. Scand. 78:318.*
12. Miller, S. D., S. J. Gerety, M. K. Kennedy, J. D. Peterson, J. L. Trotter, V. K. Tuohy, C. Waltenbaugh, M. C. Dal Canto, and H. L. Lipton. 1990. Class II-restricted T cell responses in Theiler's murine encephalomyelitis virus (TMEV)-induced demyelinating disease. III. Failure of neuroantigen-specific immune tolerance to affect the clinical course of demyelination. *J. Neuroimmunol. 26:9.*
13. Miller, S. D., R. J. Clatch, D. C. Pevear, J. L. Trotter, and H. L. Lipton. 1987. Class II-restricted T cell responses in Theiler's murine encephalomyelitis virus (TMEV)-induced demyelinating disease. I. Cross-specificity among TMEV substrains and related picornaviruses, but not myelin proteins. *J. Immunol. 138:3776.*
14. Welsh, C. J., P. Tonks, A. A. Nash, and W. F. Blakemore. 1987. The effect of L3T4 T cell depletion on the pathogenesis of Theiler's murine encephalomyelitis virus infection in CBA mice. *J. Gen. Virol. 68:1659.*
15. Gerety, S. J., M. K. Rundell, M. C. Dal Canto, and S. D. Miller. 1994. Class II-restricted T cell responses in Theiler's murine encephalomyelitis virus (TMEV)-induced demyelinating disease. VI. Potentiation of demyelination with and characterization of an immunopathologic $CD4^+$ T cell line specific for an immunodominant VP2 epitope. *J. Immunol. 152:919.*
16. Karpus, W. J., J. G. Pope, J. D. Peterson, M. C. Dal Canto, and S. D. Miller. 1995. Inhibition of Theiler's virus-mediated demyelination by peripheral immune tolerance induction. *J. Immunol. 155:947.*
17. Pope, J. G., W. J. Karpus, C. L. Vanderlugt, and S. D. Miller. 1996. Flow cytometric and functional analyses of CNS-infiltrating cells in SJL/J mice with Theiler's virus-induced demyelinating disease: evidence for a $CD4^+$ T cell-mediated pathology. *J. Immunol. 156:4050.*
18. McDonald, A. H., and R. H. Swanborg. 1988. Antigen-specific inhibition of immune interferon production by suppressor cells of autoimmune encephalomyelitis. *J. Immunol. 140:1132.*
19. Waldor, M. K., S. Sriram, R. Hardy, L. A. Herzenberg, L. Lanier, M. Lim, and L. Steinman. 1985. Reversal of experimental allergic encephalomyelitis with monoclonal antibody to a T-cell subset marker. *Science 227:415.*
20. Racke, M. K., S. Dhib-Jalbut, B. Cannella, P. S. Albert, C. S. Raine, and D. E. McFarlin. 1991. Prevention and treatment of chronic relapsing experimental allergic encephalomyelitis by transforming growth factor-β1. *J. Immunol. 146: 3012.*
21. Kennedy, M. K., D. S. Torrance, K. S. Picha, and K. M. Mohler. 1992. Analysis of cytokine mRNA expression in the central nervous system of mice with experimental autoimmune encephalomyelitis reveals that IL-10 mRNA expression correlates with recovery. *J. Immunol. 149:2496.*
22. Shaw, M. K., J. B. Lorens, A. Dhawan, R. DalCanto, H. Y. Tse, A. B. Tran, C. Bonpane, S. L. Eswaran, S. Brocke, N. Sarvetnick, L. Steinman, G. P. Nolan, and C. G. Fathman. 1997. Local delivery of interleukin 4 by retrovirus-transduced T lymphocytes ameliorates experimental autoimmune encephalomyelitis. *J. Exp. Med. 185:1711.*
23. Reiner, S. L., S. Zheng, D. B. Corry, and R. M. Locksley. 1994. Constructing polycompetitor cDNAs for quantitative PCR. *J. Immunol. Methods 173:133.*
24. Gerety, S. J., R. J. Clatch, H. L. Lipton, R. G. Goswami, M. K. Rundell, and S. D. Miller. 1991. Class II-restricted T cell responses in Theiler's murine encephalomyelitis virus-induced demyelinating disease. IV. Identification of an immunodominant T cell determinant on the N-terminal end of the VP2 capsid protein in susceptible SJL/J mice. *J. Immunol. 146:2401.*
25. Cannella, B., Y. L. Gao, C. Brosnan, and C. S. Raine. 1996. IL-10 fails to abrogate experimental autoimmune encephalomyelitis. *J. Neurosci. Res. 45:735.*
26. Mathisen, P. M., M. Yu, J. M. Johnson, J. A. Drazba, and V. K. Touhy. 1997. Treatment of experimental autoimmune encephalomyelitis with genetically modified memory T cells. *J. Exp. Med. 186:159.*
27. Vanderlugt, C. L., N. J. Karandikar, D. J. Lenschow, M. C. Dal Canto, J. A. Bluestone, and S. D. Miller. 1997. Treatment with intact anti-B7-1 mAb during disease remission enhances epitope spreading and exacerbates relapses in R-EAE. *J. Neuroimmunol. 79:113.*
28. Gerety, S. J., W. J. Karpus, A. R. Cubbon, R. G. Goswami, M. K. Rundell, J. D. Peterson, and S. D. Miller. 1994. Class II-restricted T cell responses in Theiler's murine encephalomyelitis virus (TMEV)-induced demyelinating disease. V. Mapping of a dominant immunopathologic VP2 T cell epitope in susceptible SJL/J mice. *J. Immunol. 152:908.*
29. Yauch, R. L., and B. S. Kim. 1994. A predominant viral epitope recognized by T cells from the periphery and demyelinating lesions of SJL/J mice infected with Theiler's virus is located within VP1(233–244). *J. Immunol. 153:4508.*
30. Dal Canto, M. C., R. W. Melvold, B. S. Kim, and S. D. Miller. 1995. Two models of multiple sclerosis: experimental allergic encephalomyelitis (EAE) and Theiler's murine encephalomyelitis virus (TMEV) infection—a pathological and immunological comparison. *Microsc. Res. Tech. 32:215.*
31. Ruddle, N. H. 1992. Tumor necrosis factor (TNF-α) and lymphotoxin (TNF-β). *Curr. Opin. Immunol. 4:327.*

32. Karpus, W. J., N. W. Lukacs, B. L. McRae, R. M. Streiter, S. L. Kunkel, and S. D. Miller. 1995. An important role for the chemokine macrophage inflammatory protein-1 α in the pathogenesis of the T cell-mediated autoimmune disease, experimental autoimmune encephalomyelitis. *J. Immunol. 155:5003*.
33. Karpus, W. J., and K. J. Kennedy. 1997. MIP-1α and MCP-1 differentially regulate acute and relapsing autoimmune encephalomyelitis as well as Th1/Th2 lymphoctye differentiation. *J. Leukocyte Biol. 62:681*.
34. Simmons, R. D., and D. O. Willenborg. 1990. Direct injection of cytokines into the spinal cord causes autoimmune encephalomyelitis-like inflammation. *J. Neurol. Sci. 100:37*.
35. Hsieh, C. S., S. E. Macatonia, C. S. Tripp, S. F. Wolf, A. O. O'Garra, and K. M. Murphy. 1993. Development of Th1 $CD4^+$ T cells through IL-12 produced by *Listeria*-induced macrophages. *Science 260:547*.
36. Ruddle, N. H., C. M. Bergman, K. M. McGrath, E. G. Lingenheld, M. L. Grunnet, S. J. Padula, and R. B. Clark. 1990. An antibody to lymphotoxin and tumor necrosis factor prevents transfer of experimental allergic encephalomyelitis. *J. Exp. Med. 172:1193*.
37. Powell, M. B., D. Mitchell, J. Lederman, J. Buckmeier, S. S. Zamvil, M. Graham, N. H. Ruddle, and L. Steinman. 1990. Lymphotoxin and tumor necrosis factor-α production by myelin basic protein-specific T cell clones correlates with encephalitogenicity. *Int. Immunol. 2:539*.
38. Suen, W. E., C. M. Bergman, P. Hjelmström, and N. H. Ruddle. 1997. A critical role for lymphotoxin in experimental allergic encephalomyelitis. *J. Exp. Med. 186:1233*.
39. Peterson, J. D., W. J. Karpus, R. J. Clatch, and S. D. Miller. 1993. Split tolerance of Th1 and Th2 cells in tolerance to Theiler's murine encephalomyelitis virus. *Eur. J. Immunol. 23:46*.
40. Renno, T., M. Krakowski, C. Piccirillo, J. Y. Lin, and T. Owens. 1995. TNF-α expression by resident microglia and infiltrating leukocytes in the central nervous system of mice with experimental allergic encephalomyelitis: regulation by Th1 cytokines. *J. Immunol. 154:944*.
41. Sierra, A., and N. Rubio. 1993. Theiler's murine encephalomyelitis virus induces tumour necrosis factor-α in murine astrocyte cell cultures. *Immunology 78:399*.
42. Ferber, I. A., S. Brocke, C. Taylor-Edwards, W. Ridgway, C. Dinisco, L. Steinman, D. Dalton, and C. G. Fathman. 1996. Mice with a disrupted IFN-γ gene are susceptible to the induction of experimental autoimmune encephalomyelitis (EAE). *J. Immunol. 156:5*.
43. Willenborg, D. O., S. Fordham, C. C. Bernard, W. B. Cowden, and I. A. Ramshaw. 1996. IFN-γ plays a critical down-regulatory role in the induction and effector phase of myelin oligodendrocyte glycoprotein-induced autoimmune encephalomyelitis. *J. Immunol. 157:3223*.
44. Frei, K., H. P. Eugster, M. Bopst, C. S. Constantinescu, E. Lavi, and A. Fontana. 1998. Tumor necrosis factor α and lymphotoxin α are not required for induction of acute experimental autoimmune encephalomyelitis. *J. Exp. Med. 185:2177*.
45. Liu, J., M. W. Marino, G. Wong, D. Grail, A. Dunn, J. Bettadapurs, A. J. Slavin, L. Old, and C. C. A. Bernard. 1998. TNF is a potent anti-inflammatory cytokine in autoimmune-mediated demyelination. *Nat. Med. 4:78*.
46. Tanuma, N., T. Kojima, T. Shin, Y. Aikawa, T. Kohji, Y. Ishihara, and Y. Matsumoto. 1997. Competitive PCR quantification of pro- and anti-inflammatory cytokine mRNA in the central nervous system during autoimmune encephalomyelitis. *J. Neuroimmunol. 73:197*.
47. Wogensen, L., M. S. Lee, and N. Sarvetnick. 1994. Production of interleukin 10 by islet cells accelerates immune-mediated destruction of β cells in nonobese diabetic mice. *J. Exp. Med. 179:1379*.
48. Karpus, W. J., K. E. Gould, and R. H. Swanborg. 1992. $CD4^+$ suppressor cells of autoimmune encephalomyelitis respond to T cell receptor-associated determinants on effector cells by interleukin-4 secretion. *Eur. J. Immunol. 22:1757*.
49. Chen, Y., V. K. Kuchroo, J. Inobe, D. A. Hafler, and H. L. Weiner. 1994. Regulatory T cell clones induced by oral tolerance: suppression of autoimmune encephalomyelitis. *Science 265:1237*.
50. Brocke, S., K. Gijbels, M. Allegretta, I. Ferber, C. Piercy, T. Blankenstein, R. Martin, U. Utz, N. Karin, D. Mitchell, T. Veromaa, A. Waisman, A. Gaur, P. Conlon, N. Ling, P. J. Fairchild, D. C. Wraith, A. O'Garra, C. G. Fathman, and L. Steinman. 1996. Treatment of experimental encephalomyelitis with a peptide analogue of myelin basic protein. *Nature 379:343*.
51. Mueller, R. 1997. Mechanism underlying counterregulation of autoimmune diabetes by IL-4. *Immunity 7:411*.
52. Sato, S., S. L. Reiner, M. A. Jensen, and R. P. Roos. 1997. Central nervous system cytokine mRNA expression following Theiler's murine encephalomyelitis virus infection. *J. Neuroimmunol. 76:213*.
53. Clatch, R. J., S. D. Miller, R. Metzner, M. C. Dal Canto, and H. L. Lipton. 1990. Monocytes/macrophages isolated from the mouse central nervous system contain infectious Theiler's murine encephalomyelitis virus (TMEV). *Virology 176:244*.
54. Lipton, H. L., G. Twaddle, and M. L. Jelachich. 1995. The predominant virus antigen burden is present in macrophages in Theiler's murine encephalomyelitis virus-induced demyelinating disease. *J. Virol. 69:2525*.
55. Rossi, C. P., M. Delcroix, I. Huitinga, A. McAllister, N. Van Rooijen, E. Claassen, and M. Brahic. 1997. Role of macrophages during Theiler's virus infection. *J. Virol. 71:3336*.
56. Pope, J. G., C. L. Vanderlugt, H. L. Lipton, S. M. Rahbe, and S. D. Miller. 1998. Characterization of and functional antigen presentation by central nervous system mononuclear cells from mice infected with Theiler's murine encephalomyelitis virus. *J. Virol. In press.*